Journal of the European Ceramic Society 15 (1995) 1111–1117

0955-2219(95)00086-0
0955-2219/95/$9.50

Zirconia as a Nucleating Agent in a Yttria–Alumina–Silica Glass

P. Vomacka, O. Babushkin & R. Warren

Department of Engineering Materials, Luleå University of Technology, S-951 87 Luleå, Sweden

(Received 13 February 1995; revised version received 19 May 1995; accepted 22 May 1995)

Abstract

The crystallization behaviour of a ZrO_2-containing glass and a ZrO_2-free glass in the Y_2O_3–Al_2O_3–SiO_2 system prepared at 1700°C were compared in order to study the influence of ZrO_2 on the nucleation and growth processes. Techniques used included SEM, DTA and XRD analysis. The microstructural development of the ZrO_2-containing material during crystallization was more complex than that of the ZrO_2-free material. In the crystallization treatments no phase separation prior to crystallization could be observed and no precursor crystalline phase was observed to form in the ZrO_2-containing glass. Thus the added zirconia could be considered to act as a growth modifier rather than a catalyst nucleating agent.

1 Introduction

During the sintering of Si_3N_4 materials by liquid-phase sintering an oxynitride liquid forms through reaction of oxide sintering aids (such as Y_2O_3 and Al_2O_3) with surface silica on the starting Si_3N_4 powder particles and some of the Si_3N_4. Upon cooling from the sintering temperature an intergranular glassy phase forms from the liquid. The compositions of this phase in, for example, materials with yttria and alumina as sintering aids lie within the Y_2O_3–Al_2O_3–SiO_2 system. In general, the presence of such glassy phases has a deleterious influence on the mechanical properties and oxidation behaviour of Si_3N_4 ceramics.[1–5] One approach to reducing these effects is to induce a crystallization of the amorphous phase by means of a suitable heat treatment. Experimental studies of intergranular phases to better understand their crystallization behaviour and associated property changes are difficult to perform *in situ*; for this reason it is of interest to study bulk glasses with compositions that simulate such phases.[6–10]

Nucleation catalysts are widely used in glass systems to promote crystallization. Thermal treatment at a temperature necessary for precipitation of a crystalline phase, which acts as primary nucleation centers, leads to the devitrification of the glass.[11] Another catalysis mechanism which leads to a subsequent volume crystallization and which is not yet entirely understood is phase separation leading to the formation of a fine dispersion. Phase separation can be induced by a number of oxides (such as, e.g. TiO_2 and ZrO_2).[11] Crystallization studies made by several investigators[2,12,13] have shown that ZrO_2 added to yttria–alumina–silica glasses can catalyse their crystallization.

The aim of the present work was to study the influence of ZrO_2 on crystallization of an yttria–alumina–silica glass prepared at 1700°C. The crystallization behaviour of a high Y_2O_3-content glass with and without the addition of 6 wt% zirconia was studied.

2 Experimental

The solubility limit of ZrO_2 at 1700°C in an yttrium aluminosilicate liquid with the composition of 46·9 wt% Y_2O_3, 24·3 wt% Al_2O_3 and 28·8 wt% SiO_2 was in the previous study determined as 6 wt%.[14] Therefore two glasses (A and B) with compositions x ZrO_2 + (100–x) [46·9 Y_2O_3, 24·3 Al_2O_3, 28·8 SiO_2] (where x in wt% was 0 and 6) were chosen for the present study. Both compositions were subjected to the same heat treatments as described below.

Samples were prepared from high-purity Y_2O_3, Al_2O_3, SiO_2 and unstabilized ZrO_2 powders (Rhone Poulenc, Alcoa Chemicals, Johnson Matthey Alfa Products and Sigma chemical respectively). The powders were weighed in a precision balance, mixed in polyethylene containers on a Siemens roller mill for 10 h using prophanol as mixing medium, dried and sieved. Batches of 100 g each were then mechanically compacted into molybdenum crucibles and fired in a nitrogen

Table 1. Results of heat treatment* in this study and in the previous work[14] (s is strong, m is medium, w is weak and vw is very weak)

Heat treatment		*Phase analysis*	
Time (h)	*Temp. (°C)*	*Sample A*	*Sample B*
1	900	Clear amorphous glass	Clear amorphous glass
	950	Clear amorphous glass	Clear amorphous glass
	980	Clear amorphous glass	Clear amorphous glass
	1010	Clear amorphous glass	Clear amorphous glass
	1040	Opaque amorphous glass	Clear amorphous glass
	1100	y - $Y_2Si_2O_7$, m; β - $Y_2Si_2O_7$, m; amorphous glass, w	y - $Y_2Si_2O_7$, m; amorphous phase, m
	1150[14]		y - $Y_2Si_2O_7$, s; β - $Y_2Si_2O_7$, w; Y–ZrO_2; w; $Al_6Si_2O_{13}$, vw;
	1200[14]		y - $Y_2Si_2O_7$, s; β - $Y_2Si_2O_7$, m; Y–ZrO_2; w; $Al_6Si_2O_{13}$, w
	1250[14]		β - $Y_2Si_2O_7$, s; y - $Y_2Si_2O_7$, m; Y–ZrO_2; w; $Al_6Si_2O_{13}$, w
	1300[14]		β - $Y_2Si_2O_7$, s; y - $Y_2Si_2O_7$, w; Y–ZrO_2; w; $Al_6Si_2O_{13}$, w
	1350[14]		β - $Y_2Si_2O_7$, s; y - $Y_2Si_2O_7$, w; Y–ZrO_2; w; $Al_6Si_2O_{13}$, w
6	900	Clear amorphous glass	Clear amorphous glass
	950	Clear amorphous glass	Clear amorphous glass
	980	Opaque amorphous glass	Clear amorphous glass
	1010	y - $Y_2Si_2O_7$, w; β - $Y_2Si_2O_7$, w; amorphous phase, s	Opaque amorphous glass
	1040	y - $Y_2Si_2O_7$, m; β - $Y_2Si_2O_7$, m; amorphous phase, w	y - $Y_2Si_2O_7$, m; amorphous phase, m;
	1100	y - $Y_2Si_2O_7$, s; β - $Y_2Si_2O_7$, m; amorphous phase, vw $Al_6Si_2O_{13}$, vw	y - $Y_2Si_2O_7$, s; β - $Y_2Si_2O_7$, w; amorphous phase, w; Y–ZrO_2; vw $Al_6Si_2O_{13}$, vw
12	900	Clear amorphous glass	Clear amorphous glass
	950	Clear amorphous glass	Clear amorphous glass
	980	Opaque amorphous glass	Clear amorphous glass
	1010	y - $Y_2Si_2O_7$, w; β - $Y_2Si_2O_7$, w; amorphous phase, s	Opaque amorphous glass
	1040	y - $Y_2Si_2O_7$, m; β - $Y_2Si_2O_7$, m; amorphous phase, w	y - $Y_2Si_2O_7$, m; β - $Y_2Si_2O_7$, m; amorphous phase, m
	1100	y - $Y_2Si_2O_7$, s; β - $Y_2Si_2O_7$, m; $Al_6Si_2O_{13}$, vw	y - $Y_2Si_2O_7$, s; β - $Y_2Si_2O_7$, m; Y–ZrO_2; vw; $Al_6Si_2O_{13}$, vw
	1300	β - $Y_2Si_2O_7$, s; $Al_6Si_2O_{13}$, w	β - $Y_2Si_2O_7$, s; Y–ZrO_2; m; $Al_6Si_2O_{13}$, w

*Starting materials were amorphous glasses, as evidenced by X-ray diffraction.

atmosphere (pressure of 0·17 MPa) at a temperature of 1700°C for 3 h. The heating rate up to the firing temperature was 5°C/min, the cooling rate was that given by the furnace after switching off (firing temperature to 1400°C, 20°C/min; 1400–950°C, 15°C/min and 950–500°C, 10°C/min). The furnace was a cold wall vacuum/pressure furnace with a graphite heater.

Pieces of the as-prepared glass (approximately 7 × 7 × 7 mm) were heat-treated at selected temperatures and times (see Table 1); they were placed in a Si_3N_4 powder bed in Mo crucibles and heated in a 0·17 MPa nitrogen atmosphere in the same furnace as above. The heating rate was 5°C/min and cooling was furnace cooling (see above). As-melted samples and heat-treated samples were examined by X-ray diffraction to check for crystallization and to identify crystalline phases. Powder samples of the as-melted glasses were also subjected to differential thermal analysis (DTA) at a heating rate of 10°C/min in a nitrogen atmosphere using an alumina powder reference standard. Dilatometric measurements were made on selected samples in a Netzch dilatometer 402E at a heating rate of 2°C/min. The microstructure of the samples were examined by scanning electron microscopy (SEM) using a CamScan S4-80DV instrument and attached energy dispersive spectrometer (EDS).

3 Results and Discussion

3.1 Phase identification

Crystalline phases identified by X-ray diffraction of glass cubes devitrified at temperatures between 900 and 1350°C are compiled in Table 1. These temperature limits were dictated by the measured

Table 2. Dilatometric measurements (glass transition temperatures — M_g and dilatometric softening points — M_s) and DTA measurement (the maximum of endothermic peaks indicating melting temperatures — T_L)

Sample	M_g(°C)	M_s(°C)	T_L(°C)
A	867	912	1430
B	842	900	1410, 1425*

*Two melting temperatures because of the immiscibility.[14]

glass transition temperatures and melting temperatures of the glasses (Table 2). For composition A the detected phases are in general agreement with those expected from the equilibrium phase diagram.[2,6,7,15–17] namely $Y_2Si_2O_7$ and $Al_6Si_2O_{13}$, without the appearance of the Al_2O_3 phase reported in previous studies.[6,9,14] In composition B the cubic yttria stabilized ZrO_2 ($Y–ZrO_2$) phase also appeared in all the X-ray diffraction patterns of samples heat treated at temperatures >1100°C (Fig. 1). Some unidentified phases were also detected for some heat treatments. They are probably intermediate phases and are not included in Table 1.

3.2 Microstructural changes

The EDS analysis of as-prepared glasses of both compositions revealed impurities of Fe and Mo in the microstructure probably coordinating from the starting powders and from the Mo crucibles. They appeared as small (<2 μm) particles probably of iron silicides[18] and molybdenum oxides.

Fig. 2 Glass with composition A after heat treatment at 980°C for 6 h (backscatter image—500 ×).

They influenced the crystallization process during the heat treatment to some extent but it is important to emphasize that they appeared in both glass compositions and they were of a very small amount.

At 900–950°C, no observable crystallization of composition A or B occurred. At 980°C, glass A had an opaque appearance when heat-treated for 6 and 12 h; this appeared to be due to the formation of small (1–10 μm) crystals, probably of y-$Y_2Si_2O_7$ and β-$Y_2Si_2O_7$ species (Fig. 2). They occurred to approximately the same extent for both treatment times. Their crystallization appeared to be heterogeneously nucleated by the impurities in the glass.

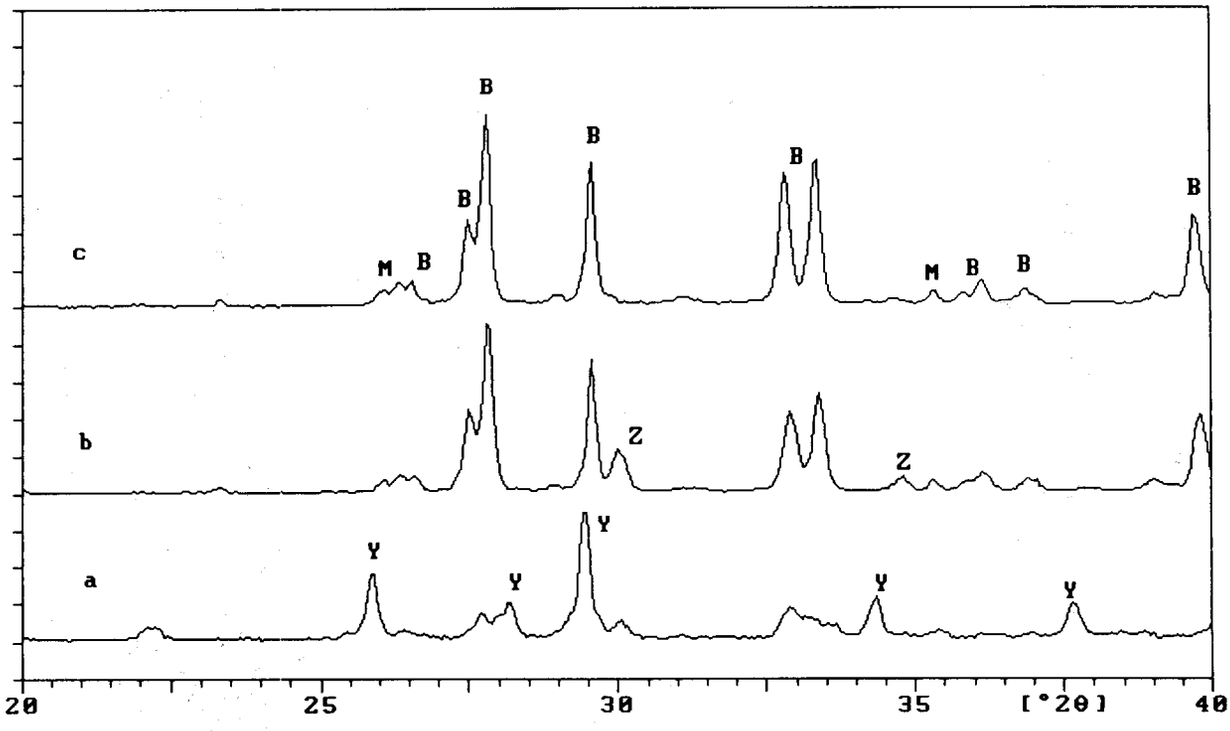

Fig. 1. X-ray diffraction patterns of the investigated glasses: (a) with 6 wt% ZrO_2 (composition B) heat treated at 1100°C for 1 h, (b) with 6 wt% ZrO_2 heat treated at 1300°C for 12 h and (c) without the addition of ZrO_2 (composition A) heat treated at 1300°C for 12 h. The symbols represent identified phases: (Y) y - $Y_2Si_2O_7$, (B) β - $Y_2Si_2O_7$, (M) mullite and (Z) cubic yttria stabilized ZrO_2. At $2\theta = 30°$ the ZrO_2 (111) peak coincides with a y - $Y_2Si_2O_7$ peak.

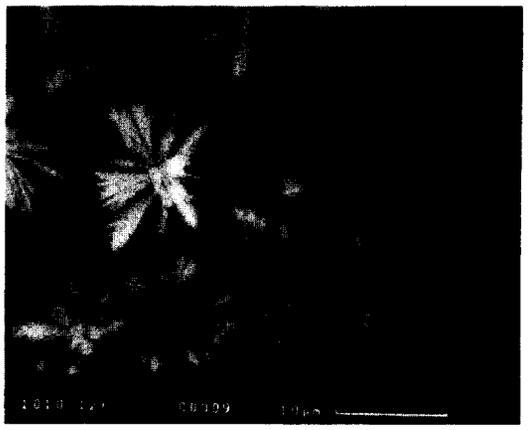

Fig. 3. Micrograph of composition A heat treated at 1010°C for 12 h with spherulitic dendrites of $Y_2Si_2O_7$ (backscatter image—2500 ×).

At 1010°C, composition A treated for 6 and 12 h exhibited an increased rate of crystallization and the occurrence of small spherulites (≈ 10–20 μm in diameter) consisting of radially growing dendrites of $Y_2Si_2O_7$ (Fig. 3). Spherulites are transient morphological forms produced during the rapid growth of crystals when the rate of growth exceeds that of diffusion and are often observed during the crystallization of highly supercooled viscous liquids. Composition B heat-treated at this temperature exhibited a similar degree of crystallization to composition A treated for 6 h at 980°C. However, in this glass the crystals were double platelike precipitates of $Y_2Si_2O_7$ in some cases with Y–ZrO_2 particles in their centers serving as nucleating catalysts (Fig. 4). These Y–ZrO_2 particles might either have been nucleated by the impurities in the glass or originated from the parent glass surviving the melting process.

At 1040°C, the crystallization rate increased for both compositions; in samples treated for 6 and 12 h the spherulites in composition A and plate crystals in composition B extended to larger dimensions (≈ 20–30 μm in diameter for spherulites and

Fig. 4. Glass B after heat treatment at 1010°C for 12 h with Y–ZrO_2 particles in centres of double platelike crystals of $Y_2Si_2O_7$ (backscatter image—2500 ×).

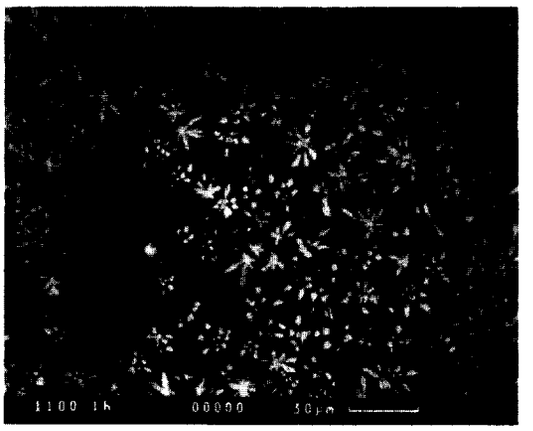

Fig. 5. Spherulites of $Y_2Si_2O_7$ in composition A after 1 h at 1100°C (backscatter image—500 ×).

20–30 μm in length for plates respectively). The microstructure of B began to be characterized by a dendritic morphology of the $Y_2Si_2O_7$. Such a morphology has been observed in the surface oxide layer of hot-pressed Si_3N_4–Y_2O_3–SiO_2 materials by Babini *et al.*[19] These authors attributed the dendrite formation to constitutional supercooling caused by a larger concentration of yttrium in the glass than in stoichiometric $Y_2Si_2O_7$. In the present case, the crystallization of y-$Y_2Si_2O_7$ requires the rejection of Al (solubility of Al in the y-$Y_2Si_2O_7$ phase decreases as a function of increasing crystallization temperature[18]), Si, O and Zr to the glass phase ahead of the glass/crystal interface. This effect would cause the constitutional supercooling resulting in dendrite formation. Glass A treated for 1 h had an opaque appearance due to a microstructure similar to those developed at 980°C after 6 and 12 h.

At 1100°C, the crystallization rate for both compositions increased dramatically with only small amounts of amorphous glassy phase retained in the microstructure (Table 1, Figs 5 and 6). The Y–ZrO_2 phase appears in the micrographs of B samples as small dendrites. In the B-glass the y-$Y_2Si_2O_7$ crystals grew to large dimensions

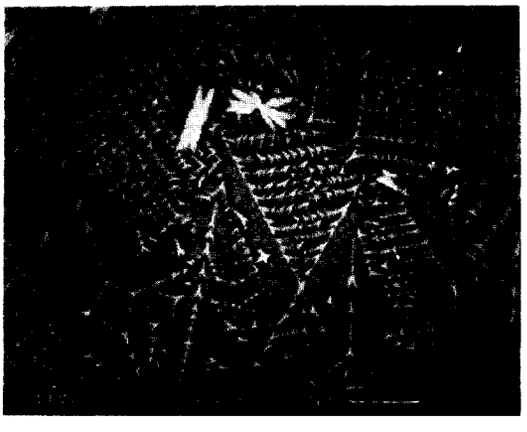

Fig. 6. Glass B after 1 h at 1100°C (backscatter image—500 ×).

Fig. 7. Crystallization of glass B at 1300°C after 12 h (backscatter image—500 ×).

presumably because they nucleated on the relatively few residual, undissolved ZrO_2 and possibly on impurity particles.

In the temperature range, 1150–1350°C (only B compositions were studied),[14] the samples were almost fully crystallized. The observations revealed different phase transformations such as crystallization of y-$Y_2Si_2O_7$, crystallization of β-$Y_2Si_2O_7$, transformation of y-$Y_2Si_2O_7$ to β-$Y_2Si_2O_7$ and crystallization of cubic yttria stabilized ZrO_2(Y–ZrO_2) occurring at different temperatures.

At 1150 and 1200°C, the microstructure of the crystallized samples was very complex with the $Y_2Si_2O_7$ occurring in the form of dendrites and fibrelike branches with an interfibrillar material which is probably amorphous.[6] At 1300°C, the y-$Y_2Si_2O_7$ phase transforms to the β-$Y_2Si_2O_7$ phase which begins to dominate the microstructure. At 1350°C, the transformation of the y-$Y_2Si_2O_7$ phase to the β-$Y_2Si_2O_7$ phase results in a β with blocky morphology to be seen growing from what were originally y-$Y_2Si_2O_7$ dendrite branches (Fig. 7). Aspects of the y $\rightarrow$ β transformation and the role of Y–ZrO_2 and its appearance in the microstructure will be discussed in the following section.

3.3 Influence of ZrO_2 on crystallization behaviour

The solubility of ZrO_2 in the investigated glass prepared at 1700°C is limited to 6 wt%.[14] As shown in Table 2 the addition of ZrO_2 leads to a decrease of the dilatometric glass transition temperature (M_g) and the dilatometric softening point (M_s) of the glass. DTA measurements on glasses with various ZrO_2 contents (0–8 wt%)[14] showed only one exothermic peak. However, this does not mean that only one crystal species is crystallizing. The broadness of the peak in ZrO_2-containing glasses indicates that ZrO_2 and other phases, mainly the $Y_2Si_2O_7$ phase, crystallize within a narrow temperature interval. The shape and lower intensity of the exothermic peak for composition B indicate a lower crystallization rate of this glass.

The crystallization of $Y_2Si_2O_7$ in composition B requires the rejection, not only of Al, Si and O but also Zr at the glass/crystal interface. The enrichment of Zr in the glass ahead of the interface would lead to a higher local viscosity of the glass near the interface than would be the case in glass A, thereby causing inhibition of the crystal growth of the $Y_2Si_2O_7$ phase. Thus, under these conditions ZrO_2 acts as a growth modifier during crystal growth.[20] The local enrichment of Zr at the glass/crystal interface might be expected to lead to the formation of ZrO_2 crystals. However, the growth of the ZrO_2 particles beyond colloidal dimensions is limited by slow diffusion of Zr in the glass at lower temperatures. In this study ZrO_2 particles growth at the glass/crystal interface was observed at higher temperatures (> 1100°C), the particles being detected by XRD and in SEM (Figs 1 and 7 and Table 1). Some of ZrO_2 remains trapped in the $Y_2Si_2O_7$ phase during cooling from the heat treatment temperature and appears as a decoration of the $Y_2Si_2O_7$ crystals in the microstructure (Fig. 8).

It has been suggested that ZrO_2 promotes liquid immiscibility because of its high cationic field strength.[21] In the present case, DTA measurements revealed two endothermic peaks in glass B around 1400°C without any mass changes occurring during the measurement.[14] They were interpreted as representing melting reactions and therefore it was concluded that the addition of ZrO_2 does enhance liquid immiscibility in this system. On the other hand, in the crystallization treatments no phase separation prior to crystallization could be observed possibly because the temperatures lay outside the appropriate range. Nevertheless, at high heat treatment temperatures (1200–1350°C) the Zr entrapped in the interfibrillar glass phase, which is rich in Al, Si and O (due to the phenomenon described above and no

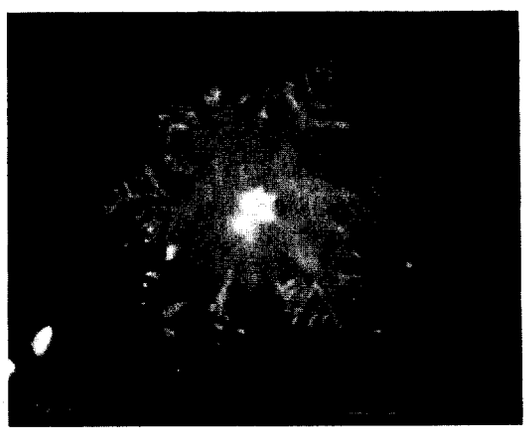

Fig. 8. Decoration of an $Y_2Si_2O_7$ crystal with ZrO_2. Composition B heat treated at 1250°C for 1 h (backscatter image—3500 ×).

Fig. 9. Zr-rich droplets in glass B heat treated at 1300°C for 1 h (backscatter image—2500 ×).

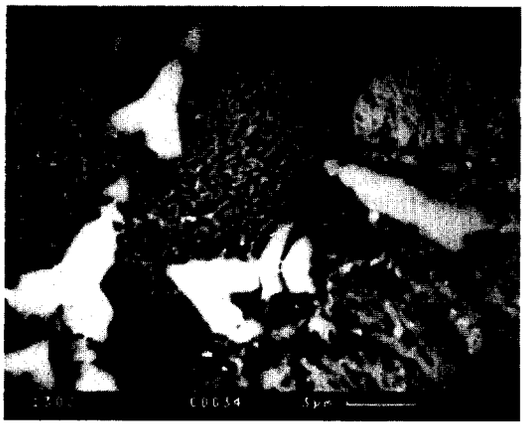

Fig. 10. Crystallization of glass B (1300°C for 1 h). Zr-rich droplets in an area that was originally y-$Y_2Si_2O_7$ fibres with the interfibrillar glass phase (backscatter image—5000 ×).

Al-containing phase having yet crystallized out) precipitated to form small Zr-rich droplets (Fig. 9). These droplets then provided nucleation sites for the β-$Y_2Si_2O_7$ and mullite crystals which then grew from the original y-$Y_2Si_2O_7$ fibres and interfibrillar glass phase (Fig. 10). Whether or not this process was initiated by phase separation[22] of the interfibrillar glass phase could not be ascertained by the available SEM analysis.

4 Conclusions

The crystallization of the ZrO_2-free glass proceeded by the formation of spherical aggregates (spherulites) consisting of radially growing dendrites. In contrast, only a small number of spherulites were observed in the ZrO_2-containing glass, the crystallization proceeding by the formation of extended dendrites rather than spherulites and being accompanied by the formation of double platelike crystals. Therefore it is believed that Zr acts as a growth modifier in this glass. As in studies of the devitrification mechanisms in $Li_2O{\cdot}Al_2O_3{\cdot}6SiO_2$ glasses[23] containing ZrO_2 as a nucleating agent, no precursor crystalline phase was observed to form in the investigated yttria–alumina–silica-glass. ZrO_2 precipitates observed in some cases, probably remaining from the glass melting, served as nucleating centers for the crystallization of the $Y_2Si_2O_7$ phase. Some of the $Y_2Si_2O_7$ crystals were probably also nucleated by impurities in the glass. The low frequency of these impurity particles and of ZrO_2 particles that survived the melting led to the formation of large $Y_2Si_2O_7$ grains. The addition of ZrO_2 might increase the rate of the y $\rightarrow$ β transformation occurring at higher temperatures compared to the ZrO_2-free glass but present results do not confirm this.

References

1. Falk, L. K. L. & Dunlop, G. L., Crystallization of the glassy phase in an Si_3N_4 material by post-sintering heat treatments. *J. Mat. Sci*, **22** (1987) 4369–76.
2. Drummond, III, Ch. H., Glass formation and crystallization in high-temperature glass-ceramics and Si_3N_4. *J. Non-Cryst. Solids.*, **123**, (1990) 114–28.
3. Kleebe, H.-J., Cinibulk, M. K., Cannon, R. M. & Ruhle, M., Statistical analysis of the intergranular film thickness in silicon nitride ceramics. *J. Am. Ceram. Soc.*, **76**(8) (1993) 1969–77.
4. Lewis, M. H., Crystallization of grain boundary phases in silicon nitride and sialon ceramics. In *Key Engineering Materials*, **89–91**, Trans Tech Publications, Switzerland, 1994, pp. 333–8.
5. Lewis, M. H., Bhatti, A. R., Lumby, R. J. & North, B. The microstructure of sintered Si–Al–O–N ceramics. *J. Mat. Sci.*, **15** (1980) 103–13.
6. Arita, I. H., Wilkinson, D. S. & Purdy, G. R., Crystallization of yttria–aluminia–silica glasses. *J. Am. Ceram. Soc.*, **75**(12) (1992) 3315–20.
7. Bondar, I. A. & Galakov, F. Ya., Phase equilibria in the system Y_2O_3–Al_2O_3–SiO_2. *Izv. Akad Nauk. SSSR Ser Khim.*, **7** (1964) 1325–6.
8. Meara, C. O., Dunlop, G. L. & Pompe, R., Phase relationship in the system Y_2O_3–Al_2O_3–SiO_2. In *Proceedings of the World Congress on High Tech Ceramics (6th CIMTEC)*, Milan, Italy, 1986, ed. P. Vincenzini, Elsevier Science Publishers, Amsterdam, pp. 265–70.
9. Hyatt, M. J. & Day, D. E., Glass properties in yttria–alumina–silica system. *J. Am. Ceram. Soc.*, **70**(10) (1987) C-283–7.
10. Loehman, R. E., Preparation and properties of oxynitride glasses. *J. Non-Cryst. Sol.*, **56** (1983) 123–34.
11. Zarzycki, J., *Glasses and the Vitreous State*. Cambridge University Press, Cambridge, 1991, 422–4.
12. Zhao, J., Wang, L., Peng, G. & Wu, J. G., Effect of zirconia on the crystallization of grain boundary. In *Proceedings of the 4th International Symposium on Ceramic Materials and Components for Engines*, Gothenburg, Sweden, 1990.
13. Thomas, G. & Ahn, C., Characterization and crystallization of Y–Si–Al–O–N glass. *Communications of the Am. Cer. Soc.* November 1982, C-185-8.
14. Vomacka, P. & Babushkin, O., Yttria–alumina–silica glasses with addition of zirconia. To be published in *J. Europ. Cer. Soc.*
15. Drummond, III, Ch. H. & Lee, W. E., Crystallization and characterization of Y_2O_3–SiO_2 glasses. *Ceram. Eng. Sci. Proc.*, **9**(9–10), (1988) 1343–54.

16. Lee, W. E., Drummond, III, Ch. H., Hilmas, G. E. & Kumar, S., Microstructural evoluation in near-eutectic yttrium silicate compositions fabricated from a bulk melt and as an intergranular phase in silicon nitride. *J. Am. Ceram. Soc.*, **73**(12) (1990) 3575–9.
17. Kumar, S. & Drummond, III, Ch. H., Crystallization of various compositions in the Y_2O_3–SiO_2 system. *J. Mater. Res.*, **7**(4) (1992).
18. Dinger, T. R., Rai, R. S. & Thomas, G., Crystallization behavior of a glass in the Y_2O_3–SiO_2–AlN system. *J. Am. Ceram. Soc.*, **71**(4) (1988) 236–44.
19. Babini, G. N., Bellosi, A. & Vincenzini, P., Factors influencing structural evolution in the oxide hot-pressed Si_3N_4–Y_2O_3–SiO_2 materials. *J. Mater. Sci*, **19** (1984) 3487–97.
20. Zdanieski, W. A., Microstructure and kinetics of crystallization of MgO–Al_2O_3–SiO_2 ceramics. *J. Am. Ceram. Soc.*, **61**(5-6) (1977) 199–204.
21. Yuan-Jang, S., Pouyan, S., San-Yuan, Ch. & Hong-Yang, L., Spherulitic growth from phase-separated vitreous matrix in a cordierite-Y-stablized zirconia glass-ceramics. *J. Am. Ceram. Soc.*, **74**(1) (1991) 85–91.
22. Aksay, I. A. & Pask, J. A., System Al_2O_3–SiO_2. *J. Am. Ceram. Soc.*, **58**(11–12) (1975) 507–12.
23. Hsu, J. & Speyer, R. F., Influences of zirconia and silicon nucleating agents on the devitrification of $Li_2O{\cdot}Al_2O_3{\cdot}6SiO_2$. *J. Am. Ceram. Soc.*, **73**(12) (1990) 3585–93.